DINOSAURIAN SURVIVORSHIP SCHEDULES REVISITED: NEW INSIGHTS FROM AN AGE-STRUCTURED POPULATION MODEL

by EVA M. GRIEBELER 🆔

Institute of Organismic & Molecular Evolution, Evolutionary Ecology, Johannes Gutenberg-University, D-55099 Mainz, Germany; em.griebeler@uni-mainz.de

Abstract: Little is known of dinosaur population biology due to insufficient information on age-dependent fecundities and mortalities. So far, survivorship curves (SC) of only six dinosaurs (four tyrannosaurs, one ceratopsian, one hadrosaur) have been erected from bone assemblages of aged specimens. They indicate high survival throughout most of their life with presumably higher mortalities after hatching and increasing mortalities towards its end. However, none of these studies recognized that to infer a reliable SC for a taxon, the assemblage must preserve a stationary age distribution (i.e. one which is stable, with constant population size over time as overall fecundities match mortalities, hereafter SAD population). To assess SCs of these dinosaurs, I built a simple population model with age-dependent fecundities and survival rates. Its three input parameters are maximum longevity, age at sexual maturation and maximum annual offspring number, for which information exists on these dinosaurs. As bone histological studies and scaling relationships provide estimates on these parameters, my model is also applicable to other extinct taxa. Modelling suggests that bone assemblages did not preserve SAD populations. SCs determined for SAD populations of *Albertosaurus sarcophagus*, *Gorgosaurus libratus*, *Dasplatosaurus torosus* and *Tyrannosaurus rex* indicated that low mortalities followed high mortalities in early life or that mortality rates were rather constant throughout their life. In *Psittacosaurus lujiatuensis*, modelling suggests low mortalities throughout most of its life that increase towards its end. Due to its simplicity, my model was unable to render composite SCs, specifically the sigmoidal shape previously predicted for *Maiasaura peeblesorum*.

Key words: life-history strategy, fecundity, stationary age-structure, attritional bone assemblage, catastrophic bone assemblage, bone histology.

AGE-SPECIFIC fecundities and mortalities determine the growth rate of a population and reveal important ecological and evolutionary insights as they reflect the life-history strategy of a species and the environment that shaped it over evolutionary time (Stearns 1992; Pianka 1999). For instance, natural selection in saturated environments favours a high intraspecific competitive ability and a low population growth rate (K-selection), whereas in heterogeneous environments intraspecific competition is reduced and a high growth rate is favoured (r-selection, Pianka 1999).

From a demographic perspective, the deaths in a population always have to be compensated for by births to enable long-term population and species survival (Stearns 1992; Pianka 1999). A female's reproductive output is age-dependent. In extant species annual fecundities can increase (e.g. fish, reptiles), decrease (e.g. small birds) with age or show a maximum within an animal's life (e.g. in large mammals and humans fecundity increases with age and shows a senescence-driven die-off towards the end of life) (Pianka 1999; Case 2000; Smith & Smith 2006).

With respect to deaths in a population, ecologists distinguish between three basic idealized curves on age-dependence of species survival ($\log_{10}$-transformed probability of surviving from birth to a given age, standardized for an initial cohort of 1000 individuals; Pearl 1928; Pearl & Minor 1935). The convex survivorship curve (type 1) assumes high survival throughout most of the life with mortalities considerably increasing towards its end. Such survivorship curves (SC) have been observed in human populations in highly industrialized countries or populations of captive animals. In contrast, species with linear SCs (type 2) show a comparatively constant mortality risk throughout their life. For small, short-lived birds, mammals and lizards, linear SCs have been found. Species with concave SCs (type 3) experience high mortalities at the beginning of their life, followed by low mortalities towards its end. SCs of large, long-lived reptiles are consistent with a concave shape (Pianka 1999; Case 2000; Smith & Smith 2006).

For a few dinosaurs, researchers have established age distributions from bone assemblages to infer their SCs.

Erickson *et al.* (2006) were the first to present dinosaurian SCs (i.e. for the North American tyrannosaurs *Albertosaurus sarcophagus*, *Dasplatosaurus torosus*, *Gorgosaurus libratus* and *Tyrannosaurus rex*). Their study followed that on the ceratopsian *Psittacosaurus lujiatunensis* from China (Erickson *et al.* 2009). The most recent is from Woodward *et al.* (2015) on the hadrosaur *Maiasaura peeblesorum* from Montana, USA. Erickson *et al.* (2010) later added four further specimens to their 2006 published *Albertosaurus sarcophagus* sample (n = 22, Erickson *et al.* 2006), but sample sizes of *Psittacosaurus lujiatunensis* (n = 80) and *Maiasaura peeblesorum* (n = 50) were still substantially larger than those of the four tyrannosaurs (*Albertosaurus sarcophagus*: n = 22, *Dasplatosaurus torosus*: n = 14, *Gorgosaurus libratus*: n = 39, *Tyrannosaurus rex*: n = 31). Erickson *et al.* (2006, 2009, 2010) derived convex SCs for tyrannosaurs and *Psittacosaurus lujiatunensis*, and hypothesized a moderate mortality rate for their first two years of life (for which they had no specimens) as seen in extant vertebrate carnivores. These authors concluded that the SCs of these species are consistent with those of long-lived birds and mammals. Woodward *et al.* (2015) established a sigmoidal-shaped SC (a moderate mortality rate in the first year of life being documented by specimens in their sample is followed by a long period of a rather constant low rates) for *Maiasaura peeblesorum*.

A few studies inspired by Erickson *et al.* (2006) aimed at improving the accuracy and biological correctness of dinosaurian SCs inferred from bone assemblages. Steinsaltz & Orzack (2011) developed a method using 95% confidence intervals around the estimated age-specific survival rates. Erickson *et al.* (2006, 2009, 2010) had applied bootstrap analysis to statistically assess inaccuracies in SCs. Steinsaltz & Orzack (2011) questioned the convex SCs hypothesized for tyrannosaurs, as they demonstrated that between 50 and 100 individuals are required for a reasonable statistical power to infer a convex SC. Ricklefs (2007) assessed aging rates (average mortality per year) from the SCs of the tyrannosaurs (Erickson *et al.* 2006) and showed that although tyrannosaurs are more closely related to birds than to mammals, their rates resembled those seen in present-day large terrestrial mammals and humans. More recently, Weon (2015) applied biodemographical analysis to the updated *Albertosaurus sarcophagus* dataset (Erickson *et al.* 2010). He challenged Ricklefs (2007) by showing that this tyrannosaur's SC was more similar to that of modern big birds than to eighteenth-century humans.

So far, all studies on dinosaurian SCs have ignored the fact that bone assemblages must comprise a stationary age distribution (i.e. the population has an age distribution which is stable in shape over time, with a size that does not change over time; hereafter SAD population); this is

required to infer reliable information on aging and even life-history strategies of species (Stearns 1992; Pianka 1999; Case 2000). It is well known that the population's growth rate affects its age distribution and vice versa (Pianka 1999; Case 2000). With respect to the stability of age distributions, Erickson *et al.* (2006) only discussed taphonomic problems for their tyrannosaur bone assemblages, that is to say, only a catastrophic assemblage (e.g. from flash floods, volcanic burial) provides a representation of the population's age distribution at a single moment (preserved individuals coexisted and deaths occurred randomly with respect to age). However, they did not note that in this situation it could indeed be possible that the population was increasing or decreasing when the catastrophic event happened. Contrary to a catastrophic assemblage, in an attritional assemblage in which the young and old individuals are the most abundant (i.e. a bimodal distribution) because they are most susceptible to mortality (Voorhies 1969), preserved individuals that did not coexist; bones are from a wide temporal and spatial range. In this case, a stationary age distribution would imply that the bone assemblage must be a sample of a population showing a constant size over the time span during which bones accumulated. This is very unrealistic given that this span could be huge, perhaps millions of years. Erickson *et al.* (2006) ruled out attritional assemblages for their tyrannosaurs as they had left-skewed age distributions (higher age classes dominate; but see Steinsaltz & Orzack 2011, who showed that a positive size-dependent fossilization rate could result in left-skewed age distributions). Conversely, Erickson *et al.* (2009) and Woodward *et al.* (2015) argued that the right-skewed age distributions of *Psittacosaurus lujiatunensis* and *Maiasaura peeblesorum* (in which younger age classes dominate) indicate that these assemblages were not attritional, because a standing crop population of the cervid *Odocoileus virginiana* had a right-skewed distribution (Voorhies 1969).

Here, I present a mathematical model for an age-structured population, using a fecundity schedule as input. Given that fecundities and mortalities determine a population's growth rate, I use the model to predict the survivorship schedule and the growth rate of a population both fitting together at best a given empirical SC under the given fecundity schedule. It thus allows a check of whether a sampled age distribution could come from a SAD population. The model is further used to calculate the SC of a SAD population given a fixed fecundity schedule. My model is very simple and designed to be applicable to extinct taxa and to assess the position of their SC within the concave to convex spectrum. It is parametrized by three life history traits only and makes use of a two-parameter family function on fecundity schedules and a one-parameter family function on the survivorship schedule. Information on the model's three input parameters maximum longevity (inferable from

their published SCs, Erickson *et al.* 2004, 2006, 2009, 2010; Woodward *et al.* 2015), age at sexual maturation (inferable from their growth curves relating age to body size, Erickson *et al.* 2001, 2009; Woodward *et al.* 2015) and maximum annual offspring number (inferable from allometric regressions relating this trait to their body mass, Werner & Griebeler 2013) is fortunately assessable for all six dinosaurs for which SCs have already been established and which are revisited herein.

First, I use my model to demonstrate how the population growth rate and fecundity schedule alter the SC of a population. Next, I apply it to 20 extant species (reptiles, birds and mammals). Specifically, I use it to check whether age distributions of sampled field populations of these species were from SAD populations and then predict their SCs given that they form SAD populations. Then I check whether the latter SCs indeed conform to literature expectations. With the first two analyses, I aim to question whether my model works for extant species and to identify sources of error when inferring SCs of extant and extinct taxa from my model.

I next show with my model that SCs established from dinosaurian bone assemblages were not from SAD populations. This result strongly questions the correctness of the previously published position of these dinosaurs within the concave to convex SC spectrum. I then use the model to determine the SCs of SAD populations of the six dinosaurs. Contrary to literature expectations, the derived SCs were concave to linear for the tyrannosaurs *Albertosaurus sarcophagus*, *Gorgosaurus libratus*, *Dasplatosaurus torosus* and *Tyrannosaurus rex*, whereas the published convex SC of *Psittacosaurus lujiatuensis* was corroborated. The model predicted a concave SC for *Maiasaura peeblesorum* which captures its high mortalities in the first years of life well, but failed to render the sigmoidal-shaped SC published by Woodward *et al.* (2015) due its simplicity.

Finally, I conclude that when good estimates on its input parameters exist, my model calculates much more reliable SCs for extinct taxa than expected from bone assemblage analysis due to the taphonomic problems of the latter.

MATERIAL AND METHOD

The model

My age-structured population model derives changes in a population's size between one year and the next from age-specific mortality and age-specific birth rates all assumed to be constant over time. It does not distinguish between individuals of different sexes and thus implicitly assumes an equal sex ratio for the population. The population's net reproductive rate (R_0) is defined as the average number of class zero offspring produced by an average newborn individual during its entire lifetime. R_0 is the sum of products of l_x and m_x:

$$R_0 = \sum_{x=0}^{\infty} l_x m_x \qquad (1)$$

where age x is a natural number (years), l_x the probability that an individual survives from birth ($x = 0$) to a given age x (>0) and m_x the number of births given by an individual of age x (within one year).

Once a population has attained a stable age distribution, R_0 equals the geometric growth rate. When R_0 is greater than one, the population is exponentially increasing, when R_0 equals one, it is constant in size (i.e. it is a SAD population), and when R_0 is smaller than one, the population is exponentially decreasing (Stearns 1992; Pianka 1999; Case 2000). My simple population model ignores fluctuations in the population's growth rate R_0 caused by environmental factors (e.g. weather, predators) that alter fecundities and mortalities over time. In natural populations R_0 values larger or smaller than one are only realized for short time periods and no population is able to exponentially increase or decrease forever. Thus averaged across time there is no growth in a population.

Modelling of age-specific survival (l_x). I used a function for age-specific survival rates l_x that is able to capture the shape of each of the three generalized SCs (convex, linear, concave; Pearl 1928; Pearl & Minor 1935). To keep it as simple as possible, I parametrized it using a single parameter (l_x shape parameter, λ) directly controlling the SC's shape and thus the position of the SC within the concave to convex spectrum. Given the $\log_{10}$-transformed l_x axis, λ values around -7 yield linear shaped, larger values convex and smaller values concave shaped SCs (Fig. 1A).

$$l_x = 1 + \frac{\exp(\lambda \cdot x) - 1}{1 - \exp(\lambda)}(1 - 0.001) \qquad (2)$$

In Equation 2, λ ($\neq 0$) is this l_x shape parameter and x is the standardized age of an individual (real number, $0 \leq x \leq 1$). The raw values of ages are natural numbers and range between zero and the maximum longevity (maxL, years) observed in the population. I obtained standardized ages by dividing the raw age by maxL. The value 0.001 corresponds to one surviving individual out of an initial cohort of 1000 individuals (Pianka 1999; Case 2000).

Modelling age-specific fecundities (m_x). For age-specific fecundities m_x, I considered five different functions (m_x models). Functions relate a fecundity value m_x to an individual's age x (natural number, $0 \leq x \leq$ maxL, Fig. 1B). All functions assume $m_x = 0$ for sexually immature individuals (age $x <$ age at sexual maturation, ASM) and make use of a maximum fecundity value ($m_{max} > 0$).
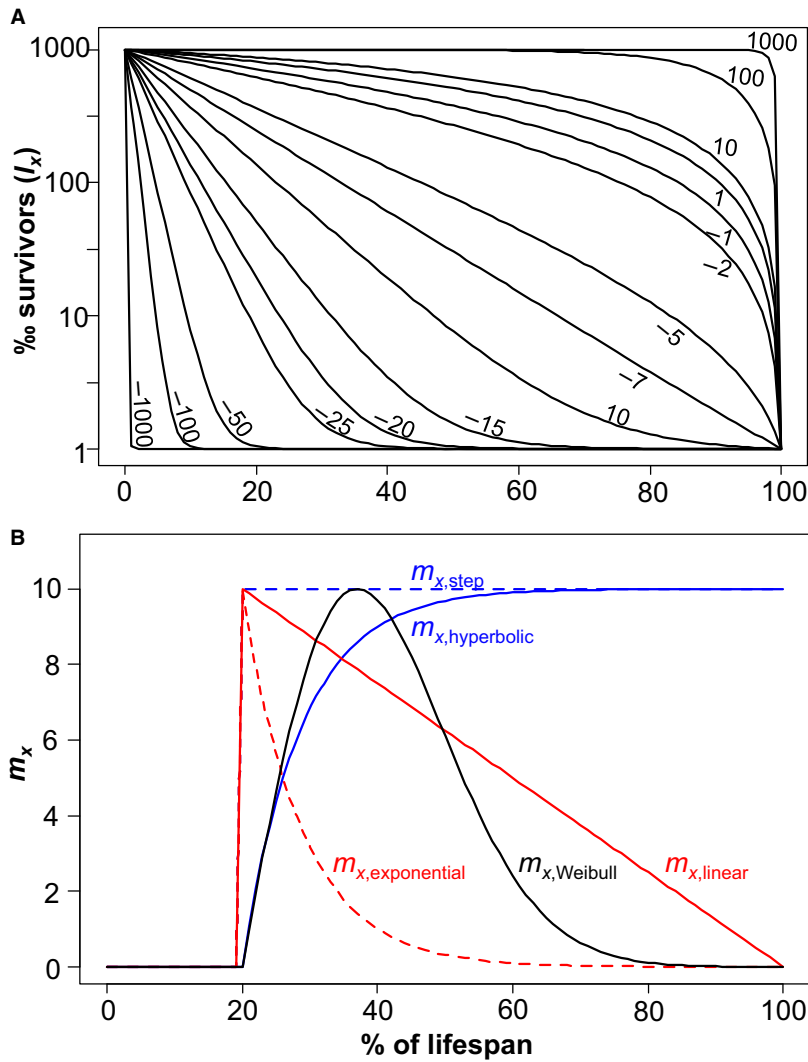
FIG. 1. The survival function (A, Eqn 2) and the five m_x models (B, Eqns 3–7) used by my age-structured population model. Age is shown as percentage of maximum longevity (% of lifespan), which was arbitrarily set to 100 (years). A, shape parameter, λ, values used by curves are indicated; age-specific survival l_x is given on a logarithmic scale for a cohort of 1000 individuals (‰ survivors); note that a linear SC is seen for λ around −7 (see main text). B, the five m_x models: $m_{x,step}$, $m_{x,hyperbolic}$, $m_{x,linear}$, $m_{x,exponential}$ and $m_{x,Weibull}$; in all models, maximum annual offspring number m_{max} was arbitrarily set to 10 and age at sexual maturation ASM to 20 years.

They cover the broad spectrum of shapes of fecundity curves found in extant animals.

The step function assumes a constant fecundity (m_{max}) after the individual has passed ASM.

$$m_{x,step} = \begin{cases} 0 & 0 \leq x < \text{ASM} \\ m_{max} & \text{ASM} \leq x \end{cases} \quad (3)$$

This is the simplest m_x model relating fecundity m_x to age ($x \geq 0$). It was suggested for several bird species (Martin 1995).

The second function establishes a hyperbolic increase in m_x for sexually mature individuals. m_{max} is the asymptote of this function:

$$m_{x,hyperbolic} = \begin{cases} 0 & 0 \leq x < \text{ASM} \\ m_{max} - m_{max} \exp\left(\dfrac{\log\left(\dfrac{0.001}{m_{max}}\right)}{\text{maxL} - \text{ASM}}(x - \text{ASM})\right) & \text{ASM} \leq x \end{cases} \quad (4)$$

The fecundity schedules of red deer studied on the island of Rhum off Scotland (Lowe 1969), of the loggerhead sea turtle (Frazer 1984) and of some birds (Martin 1995) are consistent with a hyperbolic function.

Conversely, the linear function assumes m_{max} at ASM and models a linear decrease in m_x throughout the rest of an individual's life:

$$
m_{x,\text{linear}} =
\begin{cases}
0 & 0 \leq x < \text{ASM} \\
m_{\max} - \dfrac{m_{\max}}{\text{maxL} - \text{ASM}}(x - \text{ASM}) & \text{ASM} \leq x
\end{cases}
\tag{5}
$$

White Leghorn domestic chicken (Pianka 1999) and other birds (Martin 1995) show a linear decrease in fecundity with an increasing age in their reproductive phase.

The exponential function also assumes $m_{\max}$ at ASM, but establishes an exponential decrease in m_x with increasing age for sexually mature individuals:

For insects such as the rice weevils (Birch 1948) and the

$$
m_{x,\text{exponential}} =
\begin{cases}
0 & 0 \leq x < \text{ASM} \\
m_{\max} \exp\left(\dfrac{\log\left(\dfrac{0.001}{m_{\max}}\right)}{\text{maxL} - \text{ASM}}(x - \text{ASM}) \right) & \text{ASM} \leq x
\end{cases}
\tag{6}
$$

human louse (Pianka 1999) an exponential fecundity schedule was observed.

Finally, I chose a Weibull (density) function to implement an optimum curve for age-specific fecundities for sexually mature individuals:

$$
m_{x,\text{Weibull}} =
\begin{cases}
0 & 0 \leq x < \text{ASM} \\
\dfrac{m_{\max}}{\max}\left\{ \alpha\beta^{-\alpha}(x - \text{ASM})^{\alpha-1} \exp\left(-\left(\dfrac{x - \text{ASM}}{\beta}\right)^{\alpha} \right) \right\} & \text{ASM} \leq x
\end{cases}
\tag{7}
$$

It makes use of a shape parameter $\alpha > 0$ and a scale parameter $\beta > 0$. In my formulation, the factor $(m_{\max}/\max)$, with max being the maximum value of the original Weibull function, changes this function's co-domain from $[0, \max]$ to $[0, m_{\max}]$. For my study, I chose $\alpha = 2.0$ and $\beta = 0.3 \cdot (\text{maxL} - \text{ASM})$ (Fig. 1B) as this parameter combination yields a curve similar to that which Keyfitz & Flieger (1968) observed for humans. An optimum curve on age-specific fecundities was further reported for some birds (Martin 1995) and the Asian elephant (Olsen & Wiese 2000).

Sensitivity analysis on R_0, m_{max}, ASM, m_x model with respect to SC shape

To better understand the interplay between R_0, fecundity schedules (all five m_x models are parametrized by $m_{\max}$ and ASM; see Eqns 3–7) and the shape of the SC (λ), I carried out a sensitivity analysis with my model. I inspected three growth scenarios: a shrinking population ($R_0 = 0.5$), a constant-sized population ($R_0 = 1$, i.e. a SAD population) and an increasing ($R_0 = 2$) population, for a hypothetical

species with maxL fixed to 100 years. For each of the three growth scenarios, I considered different fecundity schedules. ASM values used in fecundity schedules were 1, 5, 10 ... 95 years and $m_{\max}$ values were 5, 10 ... 100 offspring per year. Each of the combinations of ASM and $m_{\max}$ was evaluated for each of my five m_x models (Eqns 3–7). This resulted in 6000 combinations (i.e. 3 R_0; 20 ASM; 20 $m_{\max}$; 5 m_x model) for which the model was evaluated. Specifically, for each combination, I calculated with my model the λ value of the survival function (Eqn 2) by numerically solving Eqn 1 for the given R_0 value (0.5, 1.0 and 2.0) and the given fecundity schedule (ASM, $m_{\max}$, m_x model) (see below).

Application of the model to populations of extant species and dinosaurs

Extant species studied and maxL, ASM and m_{max} values used in modelling. Unlike extinct taxa, in extant species taphonomic problems with age distribution samples are absent and much better information on model parameters ASM, maxL and $m_{\max}$ exists. I, thus studied 20 extant vertebrates for which I found SCs in the literature to check whether my model can predict their SCs. These species comprised six reptiles, seven birds and seven mammals. The modelled reptiles were the desert night lizard (*Xantusia vigilis*; Zweifel & Lowe 1966), the Nile crocodile (*Crocodylus niloticus*; Blomberg *et al.* 1982), the pond slider (*Trachemys scripta*; Gibbons & Semlitsch 1982), the painted turtle (*Chrysemys picta*; Frazer *et al.* 1991), the Texas tortoise (*Gopherus berlandieri*; Hellegren *et al.* 2000) and the loggerhead sea turtle (*Caretta caretta*; Frazer 1983). All avian species studied were from Deevey (1947). These were the European robin (*Erithacus rubecula*), the song thrush (*Turdus philomelos*), the American robin (*Turdus migratorius*), the common black bird (*Turdus merula*), the common starling (*Sturnus vulgaris*), the northern lapwing (*Vanellus vanellus*) and the European herring gull (*Larus argentatus*). The mammalian species were the Dall sheep (*Ovis dalli*; Deevey 1947), the warthog (*Phacochoerus aethiopicus*; Spinage 1972), the impala (*Aepyceros melampus*; Spinage 1972), the zebra (*Equus quagga boehmi*; Spinage 1972), the African buffalo

(*Syncerus caffer*; Spinage 1972), the white-tailed deer (*Odocoileus virginianus*; Quick 1962) and the hippo (*Hippopotamus amphibious*; Millar 1988).

I further applied my model to four other vertebrate species covering the concave to convex spectrum. They were used in Erickson *et al.* (2006) as reference for dinosaurian SCs. These were the American alligator (*Alligator mississipiensis*, concave), the osprey (*Pandion haliaetus*, linear), the human (*Homo sapiens*, convex) and the African bush elephant (*Loxodonta africana*, convex).

To parametrize the survivorship function (Eqn 2) and the m_x models (Eqns 3–7) for each of these extant species, I extracted estimates for maxL, ASM and m_{max} from the papers that reported their SCs. When this was not feasible, I referred to the online database AnAge (Tacutu *et al.* 2013). Neither of these sources provided information on m_{max} for five reptiles (*Crocodylus niloticus*, *Alligator mississipiensis*, *Trachemys scripta*, *Chrysemys picta*, *Caretta caretta*) and four birds (*Erithacus rubecula*, *Turdus philomelus*, *Turdus merula*, *Vanellus vanellus*). For these reptiles, I extracted the adult body mass reported in the database AnAge (Tacutu *et al.* 2013) and then calculated the ratio of the allometrically predicted annual clutch mass and egg mass (reptile model; Eqn 8, below) to estimate m_{max} as annual fecundity. For the birds, I adopted this procedure, but applied the bird model on annual fecundity (Eqn 9, below). Sources and values of maxL, ASM and m_{max} (plus adult body mass when m_{max} was allometrically estimated) of all extant species studied are listed in (Table S1). I did not find a fecundity curve (m_x model, m_{max}, ASM) for any of the extant species in the literature and therefore considered each of my five m_x models (Eqns 3–7) for all of them.

Dinosaurs studied and maxL, ASM and m_{max} values used in modelling. I studied the four tyrannosaurs *Albertosaurus sarcophagus*, *Dasplatosaurus torosus*, *Gorgosaurus libratus* and *Tyrannosaurus rex* (Erickson *et al.* 2006, 2010), the ceratopsian *Psittacosaurus lujituensis* (Erickson *et al.* 2009) and the hadrosaur *Maiasaura peeblesorum* (Woodward *et al.* 2015). I compiled the values needed as input for my model from the literature or estimated them from the dinosaurs' adult body masses (see below). Their maximum longevities (maxL) were read off from the published SCs. For their ASM and adult body mass, I referred to published growth curves from bone histological studies (Erickson *et al.* 2001 for tyrannosaurs; Erickson *et al.* 2009 for *Psittacosaurus lujituensis*; Woodward *et al.* 2015 for *Maiasaura peeblesorum*). For an estimate of dinosaur adult body mass, I used the asymptotic body mass from its growth curve and for its ASM the age at which the curve's inflection point is seen. Evidence for inferring sexual maturity from a growth curve's inflection point exists in reptiles and amphibians (Reiss 1989; Kupfer *et al.* 2004; Lee & Werning 2008). I

estimated m_{max} of each dinosaur from its adult body mass using both the reptile and bird model from Werner & Griebeler (2013). These authors established allometries for reptiles (crocodiles and tortoises) and birds (Struthioniformes, Tinamiformes, Galliformes and Anseriformes) that relate adult body mass (BM, in g) to egg mass (EM, in g) and to annual clutch mass (ACM, in g), respectively. I then derived m_{max} as the ratio of the allometrically predicted annual clutch mass and egg mass for each dinosaur. For egg mass and annual clutch mass, Werner & Griebeler (2013) showed that in theropods (*Troodon formosus*, *Oviraptor philoceratops*, *Citipati osmolskae*, *Lourinhanosaurus antunesi*) traits conform best to those of similar-sized or scaled-up extant birds, in sauropodomorphs (*Megaloolithus patagonicus*, *Megaloolithus mammillare*, *Massospondylus carinatus*) to extant reptiles and in hadrosaurs (*Maiasaura peeblesorum*, lambeosaurine dinosaur) to both extant clades. The allometric regressions from Werner & Griebeler (2013) used for the six dinosaurs revisited herein are

Reptile model:

$$\log_{10}(\text{EM}) = -1.622 + 0.328 \cdot \log_{10}(\text{BM})$$
$$\log_{10}(\text{ACM}) = -0.695 + 0.690 \cdot \log_{10}(\text{BM}) \tag{8}$$

Bird model:

$$\log_{10}(\text{EM}) = -1.235 + 0.746 \cdot \log_{10}(\text{BM})$$
$$\log_{10}(\text{ACM}) = -0.363 + 0.726 \cdot \log_{10}(\text{BM}). \tag{9}$$

As the regression on avian egg mass (Eqn 9) against adult body mass predicts physiologically absurd egg masses for large dinosaurs, I always set egg mass to 5 kg when Equation 9 predicted a larger egg mass than 5 kg. Egg masses of the largest dinosaurs, the sauropods, are estimated to have been around 5 kg (Deeming 2006; Hechenleitner *et al.* 2016).

SCs and SAD populations. To assess whether empirical SCs of extant species and extinct dinosaurs were from SAD populations, I determined with my model for each taxon and for each of the five m_x models (Eqns 3–7, ASM and m_{max} fixed given for the species; Tables S1, S3) the combination of R_0, m_x model and λ yielding a SC fitting best to its empirical SC (for extant species erected from the sampled age distribution of the population; for dinosaurs erected from their bone assemblage). For dinosaurs studied herein, I always considered both the reptile and bird model on m_{max} (Eqns 8, 9) for each m_x model. Out of the studied dinosaurs, Werner & Griebeler (2013) had only *Maiasaura peeblesorum* in their dinosaur sample and for this hadrosaur, reproductive traits conformed more or less to both (Werner & Griebeler 2013).

Finally, I applied an Akaike information approach to establish an overall R_0 and λ value across m_x models for

each taxon. Only for dinosaurs, this was separately done for the reptile and for the bird model. Following Symonds & Moussalli (2011), I first calculated for each of the five m_x models the residual sum of squares (RSS) across all ages x ($0 \leq x \leq$ maxL) from the best SC derived under the respective m_x model (set of l_x values, values are obtained from evaluating Equation 2 for each age x assuming the best λ value, $0 \leq x \leq$ maxL, predicted l_x values) and from the empirical SC of the taxon (set of l_x values, values read off for ages x from the SC erected from the age distribution, $0 \leq x \leq$ maxL, observed l_x values). The residual value for a given age x is the difference between its observed l_x value and its predicted l_x value. For each m_x model, I then calculated the small sample size corrected AIC value (AICc) from its RSS. Next, I calculated the Akaike weight (w) from these AICc values for each of the five m_x models, which I finally used for averaging R_0 and λ values across m_x models considered for taxa.

To calculate SCs expected for SAD populations ($R_0 = 1$) of extant species and extinct dinosaurs, using my model, I calculated for each of the five m_x models the best λ value yielding a growth rate $R_0 = 1$. Only for the dinosaurs, I repeated this for both the reptile and bird model (Eqns 8, 9) on parameter m_{max} for all five m_x models.

Evaluation of the model

I implemented my age-structured population model in R (v.3.5.2; R Core Team 2018; Griebeler 2021). Numerical solving of Eqn 2 for a given R_0 value and a given fecundity schedule (ASM, m_{max}, m_x model) to determine the best λ value was done with the bisection method (Press *et al.* 1992), which is a simple root-finding-algorithm (Press *et al.* 1992).

When checking whether SCs of extant species and extinct dinosaurs come from SAD populations, R_0 was systematically altered in 0.01 steps within the interval [−25, 25] and the λ value was optimized by the bisection method for each of these R_0 values. For optimization of λ, the normalized root-mean-square deviation (RMSD) on the predicted (set of l_x values, predicted for all ages x using the λ value under consideration, $0 \leq x \leq$ maxL) and the observed SC (set of l_x values, values read off for ages x from the SC erected from the age distribution, $0 \leq x \leq$ maxL) was minimized. RMSD is the ratio of the standard deviation of the residuals (= l_x value predicted − l_x value observed for an age x, $0 \leq x \leq$ maxL) and the mean of all observed l_x values (observed l_x values of ages x are averaged over all ages x, $0 \leq x \leq$ maxL). The final best combination of R_0 and λ for the observed SC was that yielding the overall smallest RMSD value across all R_0 values and λ values evaluated. I conducted this search for the best combination of R_0 and λ fitting the observed SC in terms of minimizing RMSD for each of my five m_x models.

For estimating the λ value of a SAD population for extant species and extinct dinosaurs (of the hypothetical species in the sensitivity analysis) under a given fecundity schedule and a given m_x model, the bisection algorithm searched for the best λ value yielding R_0 for the given fecundity schedule. This procedure was again conducted for each of the five m_x models.

The initial bisection interval of λ was always [−999, 1000] (Fig. 1A). I assumed that this algorithm had converged when the bisection interval, and thus the error interval of λ, was smaller than 0.01. The final λ value was the average value of the lower and upper limit of this interval. Due to the assumed narrowness of the error interval, SCs derived for the final λ value, for the lower limit and for the upper limit were virtually identical. The bisection interval was halved in each iteration step. The accuracy of R_0 was always ±0.01.

RESULTS

Sensitivity analysis on R_0, m_{max}, ASM and m_x model used with respect to SC shape (λ)

My sensitivity analysis indicated a strong influence of both the population growth R_0 and the fecundity schedule (m_{max}, ASM, m_x model) on the shape of the SC (λ) determined from my model (Fig. 2). Given a specific combination of m_{max}, ASM and m_x model, the derived λ value was smallest for the shrinking population, intermediate for the SAD population (constant size), and highest for the increasing population. For all three R_0 scenarios, λ values decreased with increasing m_{max}. An earlier maturation within an individual's life (ASM) resulted in a smaller λ value than a later maturation. Given a specific ASM and m_{max} value, λ values were smallest for the $m_{x,step}$ and $m_{x,hyperbolic}$ models (Fig. 2A, B). They were only slightly larger for the $m_{x,linear}$ and $m_{x,Weibull}$ models than for the $m_{x,step}$ and $m_{x,hyperbolic}$ models (Fig. 2A–C, E) and they were clearly the largest for the $m_{x,exponential}$ model (Fig. 2D).

Application of the model to populations of extant species and dinosaurs

Extant species. None of the SCs of studied extant species was from a SAD population (Fig. S1) and the published age distribution samples were more or less unsuitable for assessing the position of species within the concave to convex SC spectrum. While calculated R_0 values averaged across the five m_x models indicated that populations of the reptilian species *Xantusia vigilis* ($R_0 = 0.688$), *Chrysemys picta* (0.018) and *Caretta caretta* (0.704) were shrinking, they suggested that populations of *Crocodylus*
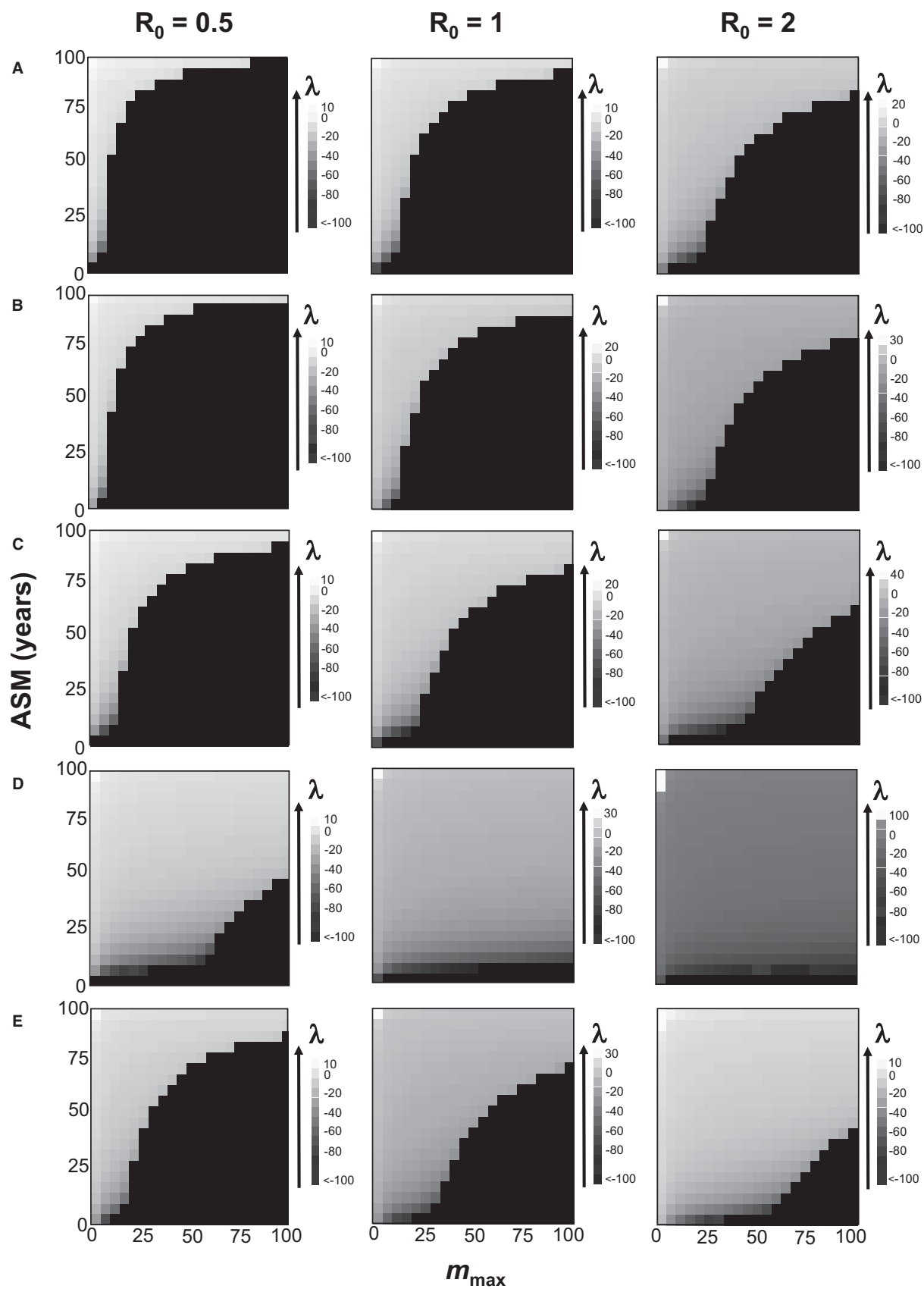
FIG. 2. Sensitivity analysis of the interplay between the fecundity schedule assumed, the population growth rate (R_0) and shape of the SC (λ). The λ value of the SC (Eqn 2) was determined for different combinations of maximum annual offspring number (m_{max}), age at sexual maturation (ASM) and R_0. Each combination of m_{max} and ASM was evaluated for each of five m_x models (rows A–E; Eqns 3–7; Fig. 1B) for a shrinking ($R_0 = 0.5$), constant-sized ($R_0 = 1$) and an increasing ($R_0 = 2$) population (the three columns). Maximum longevity was always arbitrarily set to 100 years. Models: A, $m_{x,step}$; B $m_{x,hyperbolic}$; C, $m_{x,linear}$; D $m_{x,exponential}$; E, $m_{x,Weibull}$. Arrows indicate increasing λ values and thus an increasing convexity of the derived SC. Note varying scales of λ values.

niloticus (1.389), *Trachemys scripta* (2.764) and *Gopherus berlandieri* (2.160) were increasing in size (Table S1A). When assessing their SCs in SAD populations, λ values inferred indicated a linear to convex SC, irrespective which m_x model I assumed for the species, except for *Crocodylus niloticus* (Fig. S1A; Table S2A). *Crocodylus niloticus* always had a concave SC (Fig. S1A; Table S2A).

All empirical SCs of bird species were from considerably increasing populations ($2.878 \leq R_0 \leq 7.744$), except for *Larus argentatus* (Table S1B). The latter population was comparatively slightly shrinking in size (0.884). For all bird species, SCs of SAD populations determined under the different m_x models were linear to concave, except again for *Larus argentatus* (Fig. S1B; Table S2B). The latter raptor is the largest in my sample and had a convex SC under all five m_x models.

In studied mammals, published SCs of *Phacochoerus aethiopicus* ($R_0 = 4.902$) and *Hippopotamus amphibius* (6.025) were from substantially increasing populations. Those of *Aepyceros melampus* (1.630), *Equus quagga boehmi* (1.646) and *Ovis dalli* (1.680) were from moderately increasing populations and those of *Odocoilleus virginians* (0.840) and of *Syncerus caffer* (0.364) were from shrinking populations (Table S1C).

SCs determined for SAD populations of mammals were concave to convex (Fig. S1C; Table S2C). Depending on the m_x model used, the smallest mammals in my sample *Ovis dalli*, *Phacochoerus aethiopicus* and *Aepyceros melampus* had moderately concave to slightly convex SCs and the midsized *Equus quagga boehmi* a linear to convex SC. The SCs of the largest mammal in my sample *Hippopotamus amphibius* were moderately concave to linear. The SCs of the midsized *Odocoilleus virginians* and of the large *Syncerus caffer* were clearly convex for all m_x models.

The SCs calculated for SAD populations of the four extant vertebrate species used as references for dinosaurs in Erickson *et al.* (2006) matched literature expectations (Fig. 3; Table S2D). The SC of *Homo sapiens* was convex, that of *Loxodonta africana* linear to convex, that of *Pandion haliaetus* linear to concave and that of *Alligator mississipiensis* concave.

Dinosaurs. Calculated dinosaurian R_0 indicated that bone assemblages were not from SAD populations, irrespective of whether I used a reptile or bird model on their fecundity schedule. Very large R_0 values ($15.410 \leq R_0 \leq 24.924$,

where R_0 is the mean number of offspring given per individual within its life) indicated that all bone assemblages conform to substantially increasing populations (Fig. 4; Table S3). As such R_0 values clearly contradict that bone assemblages resemble SAD populations ($R_0 = 1$) they are inadequate for drawing conclusions on the shape of the dinosaur's SC and thus of the SC's position within the concave to convex spectrum. *Psittacosaurus lujiatuensis* was the only exception. Under the bird model the best R_0 value was comparatively close to one (1.786) (Fig. 4; Table S3), whereas under the reptile model, its population was clearly increasing (8.070).

SCs calculated for dinosaurian SAD populations were linear to concave, with the bird model yielding more convex SCs than the reptile model for a given m_x model. *Psittacosaurus lujiatuensis* (Fig. 4; Table S4) was the only exception, its SC was convex under the bird and reptile model for all five m_x models considered. The updated bone assemblage on *Albertosaurus sarcophagus* (Erickson *et al.* 2010) resembled the results obtained from the somewhat smaller sample (Erickson *et al.* 2006; Fig. S2A).

DISCUSSION

Sensitivity analysis

Quality of bone assemblages for establishing SCs (SAD population). Studies so far conducted on dinosaurian SCs were only aware that bone assemblages should not be attritional (individuals coexisted) in order to avoid an overrepresentation of young and old age classes in the age distribution sample (Voorhies 1969). However, authors did not check whether assemblages were from SAD populations, that is, that the age distribution of the population is stable and the population's growth rate (R_0) equals one. My sensitivity analysis clearly shows that R_0 considerably affects the shape of the derived SC (λ). Given a fixed fecundity schedule (m_{max}, ASM, m_x model) increasing populations ($R_0 > 1$) have larger λ values and thus more convex SCs than shrinking populations ($R_0 < 1$) (Fig. 2). In increasing populations, young individuals comprise the most frequent age classes and such populations therefore have highly right-skewed age distributions, whereas those of shrinking populations are left-skewed as the older age classes dominate (Pianka 1999). Conversely, given a fixed
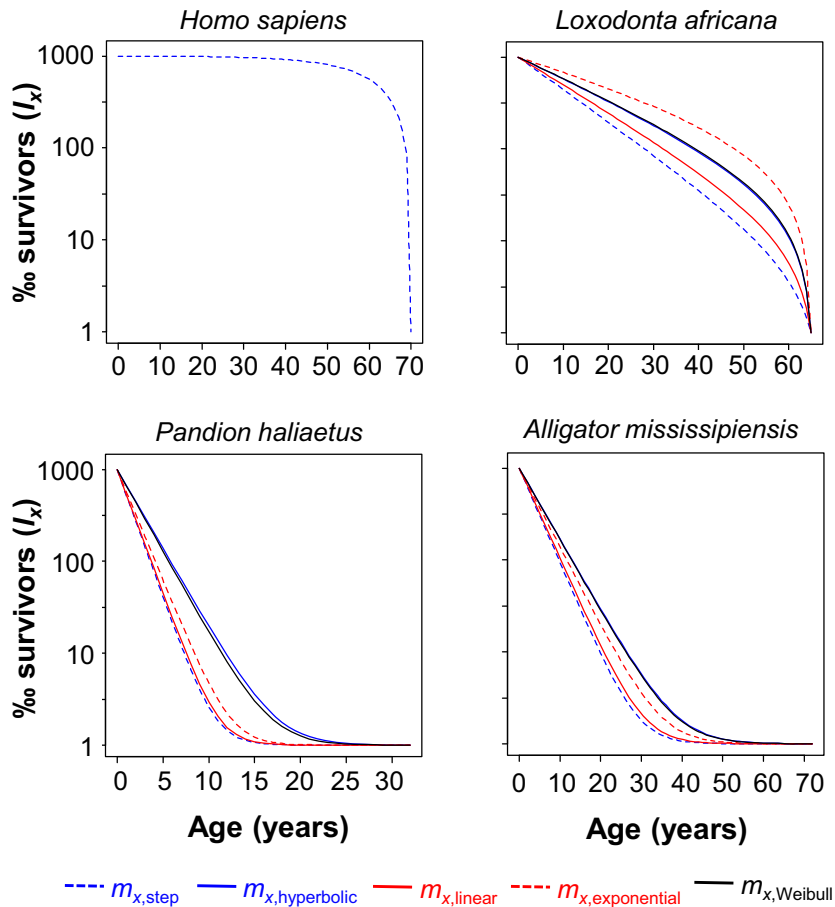
FIG. 3. Modelled SCs of SAD populations of four extant vertebrates. Species are expected to cover the complete concave (*Alligator mississipiensis*) to convex (*Homo sapiens*) SC spectrum. Each of the five m_x models ($m_{x,\text{step}}$, $m_{x,\text{hyperbolic}}$, $m_{x,\text{linear}}$, $m_{x,\text{exponential}}$, $m_{x,\text{Weibull}}$ model, Eqns 3–7; Fig. 1B) were considered for each of species. For *Homo sapiens* the bisection algorithm solving Equation 2 for $R_0 = 1$ failed to find a λ value for any m_x model except for $m_{x,\text{step}}$. Note that different m_x models can produce identical SCs (Table S2D) and then curves are overprinted. For accuracies of λ values used by SCs refer to Table S2D.

R_0 (i.e. $R_0 = 1$, a SAD population), right-skewed age distributions indicate high overall fecundities in adult age classes that result in more concave SCs, whereas left-skewed distributions indicate low fecundities that result in more convex SCs (Pianka 1999). As in fossil populations, including those of the dinosaurs studied herein (Erickson *et al.* 2006, 2009; Woodward *et al.* 2015), juveniles are most likely to be underrepresented in number, their age distributions tend to be left-skewed. Thus, as R_0 is unknown for fossil populations, their left-skewed age distribution could either indicate a shrinking population or low fecundities when assuming that the distribution is from a SAD population. In the first case the population's SC will move towards the concave end of the spectrum, whereas in the second it will move towards the convex end.

Sensitivity of calculated SCs to the fecundity schedule assumed. The modelling approach I used to check whether an age distribution is stationary (SAD population), requires most accurate fecundity schedules for the taxon. This is clearly demonstrated in my sensitivity analysis as it indicates a strong effect of m_{max}, ASM and m_x model on the λ value yielding a given overall

population growth rate R_0 (Fig. 2). The λ values decreased with increasing m_{max}, irrespective of which combination of ASM value and m_x model I assumed (Fig. 2). Parameter m_{max} sets the level of births given per individual in a population. The more births occur, the more deaths are needed to match a given R_0. The decrease in λ with increasing m_{max} implies that an overestimation of m_{max} (too large) will move a population's SC towards the concave end of the spectrum, whereas an underestimation (too small) will move it towards the convex end.

For a given m_{max} and m_x model, earlier maturation resulted in smaller λ values than those for a later maturation (Fig. 2). ASM constrains how many newborns a mature individual can potentially have within its life (the area under the age-specific fecundity curve is confined by ASM and maxL; Fig. 1B). At the population level, an early maturation results in more births than a later one and implies smaller λ values than a later maturation in order to match a given R_0. Thus, analogous to m_{max}, an overestimation of a species' ASM will move the SC towards the convex end, whereas an underestimation towards the concave end of the spectrum.

FIG. 4. Modelled SCs of the four tyrannosaurs as well as of the ceratopsian *Psittacosaurus lujiatuensis* and the hadrosaur *Maiasaura peeblesorum* using both the reptile (right column; Eqn 8) and bird (left column; Eqn 9) models on m_{max} from Werner & Griebeler (2013) and each of the five m_x models (Eqns 3–7, Fig. 1B). In each case, the SC was erected from the bone assemblage (eSC). The mSC in each plot uses the λ value derived from Akaike weights based averaging across the five m_x models. Averaged λ values were from checking whether the eSC could come from a SAD population. The SC of a SAD population ($R_0 = 1$) for each of the five m_x models (Eqns 3–7) is also shown. For detailed information on model parameter values assumed for species and modelled SCs with their accuracy, see Tables S3–S4. The model revealed very similar SCs (Fig. S2A) for the updated bone assemblage of *Albertosaurus sarcophagus* (Erickson *et al.* 2010) when compared to those derived from the original dataset (Erickson *et al.* 2006). Note that in some cases SCs are overprinted due to their very similar λ values. Silhouettes are from PhyloPic (Public Domain Dedication license (CC0 1.0); http://phylopic.org/); by Becky Barnes and Ferran Sayol, respectively.
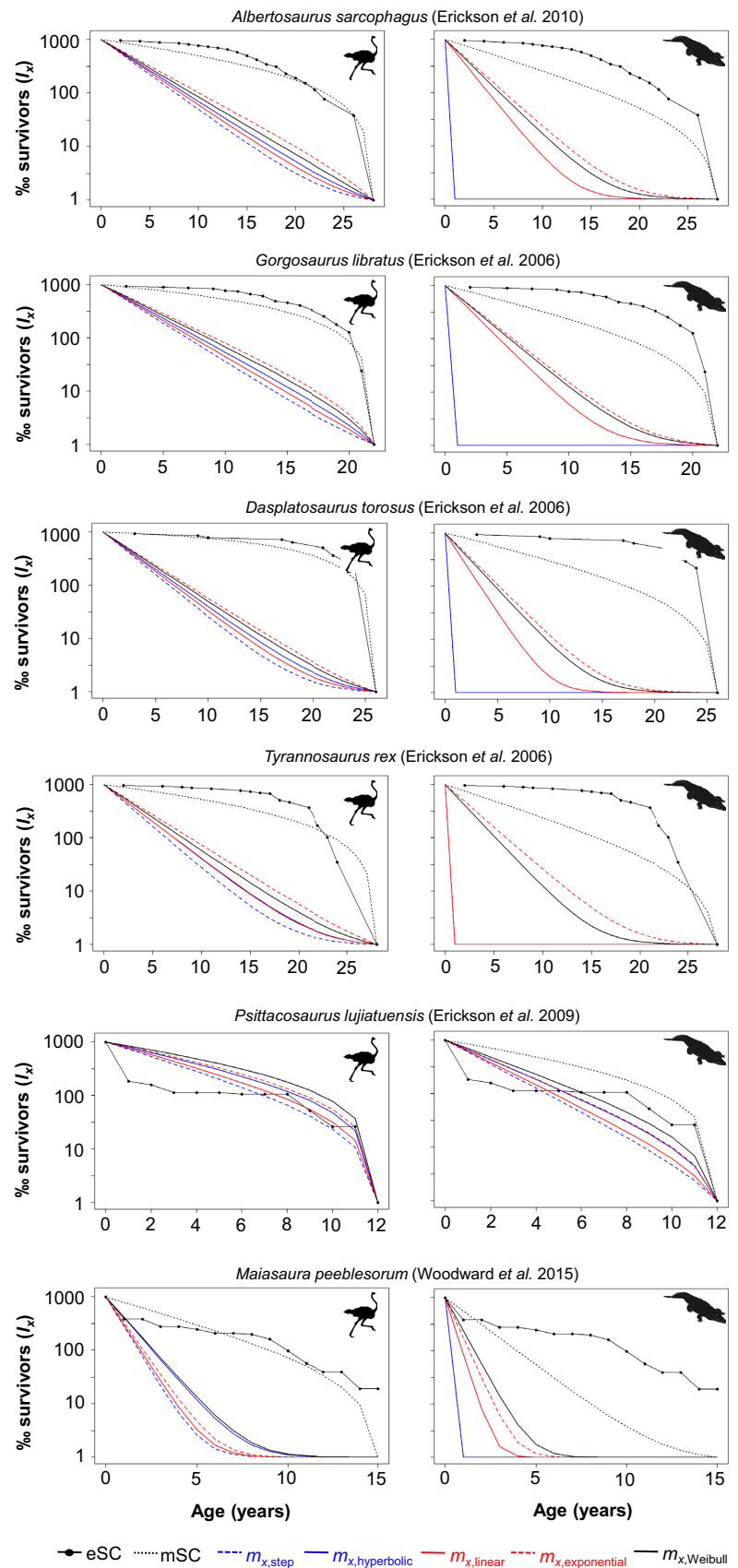
In my sensitivity analysis, the m_x model chosen also strongly affected the λ values determined for a given combination of m_{max} and ASM (Fig. 2). The λ values were smallest for the $m_{x,step}$ and $m_{x,hyperbolic}$ models, somewhat larger for the $m_{x,linear}$ and $m_{x,Weibull}$ models and were clearly the largest for the $m_{x,exponential}$ model. Given the identical m_{max} and ASM values, this ranking of m_x models reflects differences in the total number of newborns that an individual of a given age could potentially give within the rest of its life (area under the age-specific fecundity curve confined by this age and maxL; Fig. 1B). This reproductive output is highest under the $m_{x,step}$ and lowest under the $m_{x,exponential}$ model. Under the $m_{x,hyperbolic}$ model it is somewhat smaller than under the $m_{x,step}$ model and under the $m_{x,linear}$ model it is somewhat higher than under the $m_{x,Weibull}$ model. As a larger reproductive output results in more births in a population than a smaller one, deaths must be more frequent in the first situation than in the second in order to match the given R_0 of the population.

SCs of extant species and limitations on the model's applicability

Checking for SAD populations. Empirical SCs of the 20 extant species conformed best either to shrinking or increasing populations, except for *Larus argentatus* and *Odocoilleus virginians*. The R_0 value averaged across m_x models of the latter two species was much closer to one (Table S1; *Larus argentatus*: 0.884, *Odocoilleus virginians*: 0.840). Thus, even for extant species, the problem of sampling an age distribution that is from a SAD population is evident. However, field studies often reveal only a snapshot of a population's age-structure. While my model assumes that fecundities and mortalities of populations are constant over time, those of natural populations vary due to fluctuations in abiotic and biotic environmental conditions experienced by populations (e.g. weather conditions or predator abundance may vary from year to year). However, the development of methodical improvements on inferring reliable SCs for extant species is out of the scope of this study.

For one reptile (*Trachemys scripta*), six out of seven birds (all except *Erithacus rubecula*) and two out of seven mammals (*Odocoilleus virginians*, *Hippopotamus amphibius*) RMSD values were comparatively small (smaller than 0.1) and suggest a very good fit of the modelled to the empirical SC (Fig. S1; Table S1). The other 11 taxa uncover several limitations to the applicability of my model:

1. Life history traits of species are plastic with respect to environmental conditions experienced by populations

(Promislow & Harvey 1990; Ricklefs 2000; Morrison & Hero 2003; Blank & Lamouroux 2007; Parker & Andrews 2007). Finding estimates of traits parametrizing their fecundity schedules was difficult in all species. My sensitivity analysis suggests that each of these can considerable affect the shape of the SC (λ; Fig. 2).

2. My one-parameter family survival Equation 2 is unable to model composite curves of the three generalized SCs (concave, linear, convex). An implementation of such SCs requires further model parameters (e.g. the equation used in Weon & Je 2011 makes use of an age-dependent l_x shape parameter), which is particularly problematic when the number of age classes of a species is comparatively small (i.e. the species' maximum longevity (maxL) is small). *Crocodylus niloticus* and *Erithacus rubecula* had the largest RMSD values across all extant species studied (*Crocodylus niloticus*: 0.412 ≤ RMSD ≤ 0.431, *Erithacus rubecula*: 0.216; Table S1). Their empirical SCs show a concave phase at the beginning of their life, followed by a linear phase in the middle and an exponential phase towards the end of their life (Fig. S1).

3. For nine species, a further important source of error is that the maximum longevity from the empirical SC is clearly smaller than their true maximum longevity. This was seen in four reptiles (*Xantusia vigilis*, *Trachemys scripta*, *Gopherus berlandieri*, *Caretta caretta*) and five mammals (*Phacochoerus aethiopicus*, *Aepyceros melampus*, *Equus quagga boehmi*, *Syncerus caffer*, *Hippopotamus amphibius*). Their true SCs will be more convex than the ones determined from my model herein.

Calculated SCs of SAD populations. Nevertheless, given all the limitations listed above, SCs of SAD populations modelled for extant species matched more or less well literature expectations with respect to their position within the concave to convex spectrum (Figs S1, S3).

In reptiles, modelled curves were linear to convex, except for *Alligator mississipiensis* and *Crocodylus niloticus* (with the composite empirical SC). The concave SC observed for *Alligator mississipiensis* (irrespective which m_x model I assumed) is consistent with the observation that the largest reptiles show concave SCs, whereas small and short-lived reptiles have linear SCs (Pianka 1999; Case 2000; Smith & Smith 2006). Indeed, for all m_x models my results predicted a linear SC for the small-sized tortoises *Trachemys scripta* and *Chrysemys picta* as well as for the mid-sized tortoise *Gopherus berlandieris*. For the small lizard *Xantusia vigilis* and the very large turtle *Caretta caretta* it is likely that the substantial underestimation of their true maximum longevity explains their unexpected convex shaped SCs (Fig. S1A).

For all bird species, modelled SCs were concave, except for *Larus argentatus* and *Turdus migratorius* (Fig. S1B). *Larus argentatus* was the largest bird in my sample and had a convex SC under all m_x models, whereas that of the similar-sized, but longer-lived *Pandion haliaetus* were always concave (Fig. 3; Table S2D). For *Turdus migratorius*, a linear SC was only found for the $m_{x,Weibull}$ model, whereas those derived from all other m_x models were concave. Contrary to all other bird species studied, the raptor *Larus argentatus* matures late compared to its maximum life span (in the middle of its maximum lifespan) and has a low annual fecundity (three eggs; Table S1). This is consistent with a more K-selected life-history strategy in this raptor and with the convex SC calculated for this species. The five songbirds studied and *Vanellus vanellus*, however, become sexually mature in their first or second year of life (maximum longevities are between 7 and 12 years; Table S1) and show a considerably higher fecundity (7 up to 12 eggs; Table S1) than *Larus argentatus*. This indicates a more r-selected life-history strategy and a more concave SC for all six of these bird species. Early reproduction within life also questions the correctness of the $m_{x,Weibull}$ model yielding a linear SC for *Turdus migratorius*, whereas the $m_{x,step}$ and $m_{x,linear}$ model yielded a concave SC is corroborated in small birds (Martin 1995; Pianka 1999). Given that the SC plotted in Erickson *et al.* (2006) was erected from a SAD population, the other raptor (*Pandion haliaetus*) indicates a substantial mortality during the early phase of its life (concave), a broad linear phase in the middle of life, and a short convex phase towards its end. The survivorship function of my model (Eqn 2) is unable to capture such a complex survivorship schedule.

From the literature (Pianka 1999; Case 2000; Smith & Smith 2006), I expected a linear SC for the small, short-lived mammals and a convex SC for the large mammals. The smallest mammals in my sample (*Ovis dalli*, *Phacochoerus aethiopicus* and *Aepyceros melampus*) had moderately concave to slightly convex SCs and the midsized *Equus quagga boehmi* a linear to convex SC depending on the m_x model used. The SCs of the midsized *Odocoilleus virginians* and of the large *Syncerus caffer* were clearly convex. *Homo sapiens* had a convex SC and that calculated for *Loxodonta africana* was convex, too. The SCs modelled for the large *Hippopotamus amphibius* were moderately concave to linear. Thus, all predicted SCs of mammals conform to literature expectations (Fig. 3; Fig. S1), except for *Hippopotamus amphibius*. The life table in Millar (1988) used in my study on the hippo lacks information on survival of individuals of ages less than than four years (Fig. S1) and does not show the high mortalities between birth and one year (45%; Owen-Smith 1992) reported for this species. These high mortalities of young indicate that the true SC of this species is again a composite curve.

SCs of the six dinosaurs studied

I next applied my model to the six dinosaurs subject to this study (Erickson *et al.* 2006, 2009, 2010; Woodward *et al.* 2015). Modelling clearly demonstrated that dinosaur bone assemblages were from substantially increasing populations ($8.070 \leq R_0 \leq 24.924$) and that they had not preserved SAD populations. The only exception was seen for *Psittacosaurus lujiatuensis* under the bird model on m_{max} for which my model yielded a R_0 value comparatively close to one (1.786). For *Psittacosaurus lujiatuensis*, the SC of the SAD population was convex under both the bird and reptile model for all m_x models corroborating Erickson *et al.* (2009). For all of the other five dinosaurs, SCs calculated for SAD populations were linear to concave, with the reptile model resulting in more concave SCs than the bird model. Linear to concave SCs derived herein contradict fairly convex (tyrannosaurs; Erickson *et al.* 2006, 2010) and sigmoidal-shaped SCs (*Maiasaura peeblesorum*; Woodward *et al.* 2015) published for these dinosaurs before.

When checking for SAD populations, dinosaurian λ values were always smaller under the reptile than under the bird model on m_{max} (Tables S3, S4), which is consistent with the larger annual egg numbers (m_{max}) seen in similar-sized reptiles than in birds and the results of my sensitivity analysis (Fig. 2). Changing the m_x model for a dinosaur altered modelled λ values less than applying a reptile or a bird model on m_{max} (Fig. 4). All these observations stress again the need for precise fecundity schedules with which to assess dinosaurian SCs but such information on dinosaur taxa is generally rare or simply not preserved in the fossil record (e.g. number of clutches per year). Except for *Maiasaura peeblesorum*, for none of the six dinosaurs studied herein egg masses or clutches sizes are known and for all including *Maiasaura peeblesorum* the best allometric model on annual egg number is unknown (Werner & Griebeler 2013). On the other hand, at least for inferring dinosaurian ASM from growth curves reliable evidence exists. Histological studies reported medullary bone, a distinct indicator of reproductive maturity, in several dinosaurs. This ephemeral bony tissue forms before ovulation in the marrow cavities of birds as a calcium source for eggshelling. It was described in a single specimen of the tyrannosaur *Tyrannosaurus rex* (Schweitzer *et al.* 2005), in another saurischian dinosaur, *Allosaurus*, and in the iguanodontid *Tenontosaurus* (Lee & Werning 2008). Lee & Werning (2008) showed for these three taxa that ages at reproductive maturity as indicated by medullary bone coincide with ages at which growth acceleration turns into deceleration (inflection point of the growth curve). These authors further concluded a reptile-like reproduction strategy (reproductive maturity occurs while growth continues) and ruled out a bird-like strategy (reproductive maturity occurs after growth has stopped) for the three taxa. They further argued

that the strong correlation in amniotes between relatively early reproduction and high adult mortality (Tinkle *et al.* 1970; Promislow & Harvey 1990, 1991) suggests that all these extinct taxa also experienced a high adult mortality. Thus, the concave SCs that I determined under a reptile model for all dinosaurs add further support to a reptile-like reproduction strategy at least in *Tyrannosaurus rex*. However, some medium and large-sized mammals also start to reproduce before being fully-grown (e.g. female elephants; Owen-Smith 1992) but similar-sized reptiles become sexually mature later than similar-sized mammals (Hallmann & Griebeler 2018) and usually have lower maximum longevities than similar-sized mammals (Western & Ssemakula 1982; Hallmann & Griebeler 2018). Reptiles must thus have higher annual offspring numbers than similar-sized mammals (Werner & Griebeler 2011, 2013) in order to balance deaths by births in a population ($R_0 = 1$). Further, a mammalian aging and reproduction strategy (as suggested by Ricklefs 2007) leading to a convex SC is unlikely in tyrannosaurs as both the reptile and the bird models (Eqns 8, 9) reveal higher annual egg numbers than a mammal model for large similar-sized species (Werner & Griebeler 2011; Hallmann & Griebeler 2018).

Concave to linear SCs obtained for *Maiasaura peeblesorum* under the reptile and bird model are consistent with the high mortality within the first year of life (89.9%) observed by Woodward *et al.* (2015). For this hadrosaur, these authors further suggested that the early high mortality (concave shape) is followed by a period of low mortality (linear to convex shape), the latter eventually ending in senescent attrition (note maximum longevity is not documented in their sample). On the one hand my survivorship function (Eqn 2) is unable to capture the situation of having concave, linear or convex shapes at different phases within an animal's life and thus my model is unable to directly check the conclusion of Woodward *et al.* (2015). The composite curve suggested by these authors is consistent with the comparatively large RMSD values derived from my model (Table S3). On the other hand, my model suggests that the SC erected by these authors was from a substantially increasing population ($21.223 \leq R_0 \leq 24.704$; Table S3) and thus indicates that young individuals are clearly overrepresented in their bone assemblages. This artefact might question whether this hadrosaur really experienced two different phases of mortality at the beginning of its life. A larger maximum longevity than that documented in the bone assemblage would move the SC of *Maiasaura peeblesorum* calculated by my model towards the convex end of the spectrum.

Out of my dinosaur sample, the small ceratopsian *Psittacosaurus lujiatuensis* had clearly convex SCs under the bird model, whereas the SCs from the reptile model were less, but still convex (Fig. 4). For this dinosaur Zhao *et al.* (2013) reported a juvenile-only cluster with clear evidence

of different ages (five 2-year olds and one 3-year old). Authors interpreted it as a close-knit, mixed-age herd either for protection against predators or as putative helpers at the parental nest. The more or less convex SCs inferred from my model indicate low mortalities within the first years of life in *Psittacosaurus lujiatuensis*, which are consistent with both interpretations of this cluster (Zhao *et al.* 2013).

CONCLUSION

This study presents an age-structured population model to assess age-specific survival and even life-history strategies of dinosaurian taxa when making assumptions about their age-specific fecundities. As information on dinosaurian survivorship and fecundity schedules is scarce, it only makes use of three life-history traits (maximum longevity, age at sexual maturation, maximum annual offspring number), two-parameter family equations on fecundity schedules and a one-parameter family equation on the survival schedule. My sensitivity analysis shows that the accuracy of an inferred SC depends considerably on the model parameter values used and the m_x model chosen. Bone assemblages of all six dinosaurs revisited herein clearly did not preserve SAD populations (except for *Psittacosaurus* under the bird model on maximum annual offspring number) and were thus inadequate for inferring their SCs. As bone assemblages are unlikely to be from a constant-sized population, the application of my model is a much better approach to assess the position of dinosaurian SCs within the concave to convex spectrum, given that good estimates of model input parameters are available. Fortunately, information on the three life-history traits used by my model is steadily increasing from bone histological studies and the discovery of new fossils. My results strongly question published fairly convex SCs on the four tyrannosaurs (Erickson *et al.* 2006, 2010) and a K-selected life-history strategy with low fecundities suggested for them previously. It provides further evidence of a reptile-like reproduction strategy in *Tyrannosaurus rex* (Lee & Werning 2008) and for a convex SC in *Psittacosaurus lujiatuensis* (Erickson *et al.* 2009). The position of *Maiasaura peeblesorum* within the concave to convex SC spectrum could not be successfully evaluated as its bone assemblage suggests a (sigmoidal) composite SC (Woodward *et al.* 2015).

DATA ARCHIVING STATEMENT

Data for this study including all R scripts used for modelling dinosaurs and extant species are available in the Dryad Digital Repository: https://doi.org/10.5061/dryad.5mkkwh765

Editor. Kenneth Angielczyk

SUPPORTING INFORMATION

Additional Supporting Information can be found online (https://doi.org/10.1111/pala.12576):

Fig. S1. Modelled survivorship curves of six extant reptiles (A), seven birds (B) and seven mammals (C).

Table S1. Modelling results on whether empirical survivorship curves of six extant reptile, seven bird, and seven mammal species are from SAD populations.

Table S2. Survivorship curves modelled for SAD populations of studied extant reptiles, birds and mammals.

Fig. S2. Modelled survivorship curves of the four tyrannosaurs *Albertosaurus sarcophagus*, *Gorgosaurus libratus*, *Dasplatosaurus torosus*, *Tyrannosaurus rex* (A), and of the ceratopsian *Psittacosaurus lujiatuensis* and the hadrosaur *Maiasaura peeblesorum* (B).

Table S3. Modelling results on whether bone assemblage based survivorship curves of the six dinosaurs studied are from SAD populations.

Table S4. Survivorship curves modelled for SAD populations of studied six dinosaurs.

REFERENCES

BIRCH, L. C. 1948. The intrinsic rate of natural increase of an insect population. *Journal of Animal Ecology*, **16**, 15–26.

BLANK, A. and LAMOUROUX, N. 2007. Large-scale intraspecific variation in life-history traits of European freshwater fish. *Journal of Biogeography*, **34**, 862–875.

BLOMBERG, G. E. D., PIERRE, B. C., ST. SMITH, K. D., CADELL, S. M. and PETT, S. R. 1982. Simulated population dynamics of crocodiles in the Okavango river, Botswana. 343–375. *In* RHODA, B., DIETZ, D. and WAYNE, K. F. (eds). *Crocodiles: Proceedings of the fifth working meeting of the IUCN SSC Crocodile Specialist Group*. 409 pp.

CASE, T. J. 2000. *An illustrated guide to theoretical ecology*. Oxford University Press, 449 pp.

DEEMING, D. C. 2006. Ultrastructural and functional morphology of eggshells supports the idea that dinosaur eggs were incubated buried in a substrate. *Palaeontology*, **49**, 171–185.

DEEVEY, E. S. Jr 1947. Life tables of natural populations of animals. *The Quarterly Review of Biology*, **22**, 283–314.

ERICKSON, G. M., ROGERS, K. R. and YERBY, S. A. 2001. Dinosaurian growth patterns and rapid avian growth rates. *Nature*, **412**, 429–432.

ERICKSON, G. M., MAKOVICKY, P. J., CURRIE, P. J., NORELL, M. A., YERBY, S. A. and BROCHU, C. A.

2004. Gigantism and comparative life-history parameters of tyrannosaurid dinosaurs. *Nature*, **430**, 772–775.

ERICKSON, G. M., CURRIE, P. J., INOUYE, B. D. and WINN, A. A. 2006. Tyrannosaur life tables: an example of nonavian dinosaur population biology. *Science*, **313**, 213–217.

ERICKSON, G. M., MAKOVICKY, P. J., INOUYE, B. D., ZHOU, C.-F. and GAO, R.-Q. 2009. A life table for *Psittacosaurus lujiatunensis*: initial insights into ornithischian dinosaur population biology. *The Anatomical Record*, **292**, 1514–1521.

ERICKSON, G. M., CURRIE, P. J., INOUYE, B. D. and WINN, A. A. 2010. A revised life table and survivorship curve of *Albertosaurus sarcophagus* based on the Dry Island mass death assemblage. *Canadian Journal of Earth Science*, **47**, 1269–1275.

FRAZER, N. B. 1983. Survivorship of adult female loggerhead sea turtles, *Caretta caretta*, nesting on Little Cumberland Island, Georgia, USA. *Herpetologica*, **39**, 436–447.

FRAZER, N. B. 1984. A model for assessing mean age-specific fecundity in sea turtle populations. *Herpetologica*, **40**, 281–291.

FRAZER, N. B., GIBBONS, J. W. and GREENE, J. L. 1991. Growth, survivorship and longevity of painted turtles *Chrysemys picta* in a Southwestern Michigan marsh. *The American Midland Naturalist*, **125**, 245–258.

GIBBONS, J. W. and SEMLITSCH, R. D. 1982. Survivorship and longevity of a long-lived vertebrate species: how long do turtles live? *Journal of Animal Ecology*, **51**, 523–527.

GRIEBELER, E. M. 2021. Data from: Dinosaurian survivorship schedules revisited: new insights from an age-structured population model. *Dryad Digital Repository*. https://doi.org/10.5061/dryad.5mkkwh765

HALLMANN, K. and GRIEBELER, E. M. 2018. An exploration of differences in the scaling of life history traits with body mass within reptiles and between amniotes. *Ecology & Evolution*, **8**, 5480–5494.

HECHENLEITNER, M., FIORELLI, L. E., GRELLET-TINNER, G., LEUZINGER, L., BASILICI, G., TABORDA, J. R. A., DE LA VEGA, S. R. and BUSTAMANTE, C. A. 2016. A new upper Cretaceous titanosaur nesting site from La Rioja (NW Argentina), with implications for titanosaur nesting strategies. *Palaeontology*, **59**, 433–446.

HELLEGREN, E. C., KAZMAIER, R. T., RUTHVEN, D. C. III and SYNATZSKE, D. R. 2000. Variation in tortoise life history: demography of *Gopherus berlandieri*. *Ecology*, **81**, 1297–1310.

KEYFITZ, N. and FLIEGER, W. 1968. *World population: An analysis of vital data*. University of Chicago Press, 686 pp.

KUPFER, A., NABHITABHATA, J. and HIMSTEDT, W. 2004. Reproductive ecology of female caecilian amphibians (genus *Ichthyophis*): a baseline study. *Biological Journal of the Linnean Society*, **83**, 207–217.

LEE, A. H. and WERNING, S. 2008. Sexual maturity in growing dinosaurs does not fit reptilian growth models. *Proceedings of the National Academy of Sciences*, **105**, 582–587.

LOWE, V. P. W. 1969. Population dynamics of red deer (*Cervus elaphus* L.) on Rhum. *Journal of Animal Ecology*, **38**, 425–457.

MARTIN, K. 1995. Patterns and mechanisms for age-dependent reproduction and survival in birds. *American Zoologist*, **35**, 340–348.

MILLAR, A. R. 1988. A set of test life tables for theoretical gerontology. *Journal of Gerontology*, **43**, B43–B49.

MORRISON, C. and HERO, J.-M. 2003. Geographic variation in life-history characteristics of amphibians: a review. *Journal of Animal Ecology*, **72**, 270–279.

OLSEN, D. and WIESE, R. J. 2000. State of the North American elephant population and projections for the future. *Zoo Biology*, **19**, 311–320.

OWEN-SMITH, R. N. 1992. *Megaherbivores: The influence of very large body size on ecology*. Cambridge University Press, 388 pp.

PARKER, S. L. and ANDREWS, R. M. 2007. Incubation temperature and phenotypic traits of *Sceloporus undulates*: implications for the northern limits of distribution. *Oecologia*, **151**, 218–231.

PEARL, R. 1928. *The rate of living*. Knopf, 224 pp.

PEARL, R. and MINOR, J. R. 1935. Experimental studies on the duration of life. XIV. The comparative mortality of certain lower organisms. *The Quarterly Review of Biology*, **10**, 60–79.

PIANKA, E. R. 1999. *Evolutionary ecology*. Sixth edition. Pearson Education, 512 pp.

PRESS, W. H., TEUKOLSKY, S. A., VETTERLING, W. T. and FLANNERY, B. P. 1992. *Numerical recipes in C: The art of scientific computing*. Cambridge University Press, 1032 pp.

PROMISLOW, D. E. L. and HARVEY, P. H. 1990. Living fast and dying young: a comparative analysis of the life history variation among mammals. *Journal of Zoology*, **220**, 417–437.

PROMISLOW, D. E. L. and HARVEY, P. H. 1991. Mortality rates and the evolution of mammal life histories. *Acta Oecologica*, **12**, 119–137.

QUICK, H. F. 1962. Population dynamics of the white-tailed deer. 63–75. *In* BAKER, M. F. (ed.) *Proceedings of the first national white-tailed deer disease symposium*. 202 pp.

R CORE TEAM. 2018. *R: a language and environment for statistical computing*. R Foundation for Statistical Computing. https://www.R-project.org

REISS, M. J. 1989. *The allometry of growth and reproduction*. Cambridge University Press, 182 pp.

RICKLEFS, R. E. 2000. Density dependence, evolutionary optimization, and the diversification of avian life histories. *The Condor*, **102**, 9–22.

RICKLEFS, R. E. 2007. Tyrannosaur aging. *Biology Letters*, **3**, 214–217.

SCHWEITZER, M. H., WITTMEYER, J. L. and HORNER, J. R. 2005. Gender-specific reproductive tissue in ratites and *Tyrannosaurus rex*. *Science*, **308**, 1456–1460.

SMITH, T. M. and SMITH, R. L. 2006. *Elements of ecology*. Pearson Education, 719 pp.

SPINAGE, C. A. 1972. African ungulate life tables. *Ecology*, **53**, 645–652.

STEARNS, S. C. 1992. *The evolution of life histories*. Oxford University Press, 264 pp.

STEINSALTZ, D. and ORZACK, S. H. 2011. Statistical methods for paleodemography on fossil assemblages having small numbers of specimens: an investigation of dinosaur survival rates. *Paleobiology*, **37**, 113–125.

SYMONDS, M. R. E. and MOUSSALLI, A. 2011. A brief guide to model selection, multimodal inference and model averaging in behavioural ecology using Akaike's information criterion. *Behavioral Ecology & Sociobiology*, **65**, 13–21.

TACUTU, R., CRAIG, T., BUDOVSKY, A., WUTTKE, D., LEHMANN, G., TARANUKHA, D., COSTA, J., FRAIFELD, V. E. and MAGELHAES, J. P. 2013. Human ageing genomic resources: integrated databases and tools for the biology and genetics of ageing. *Nucleic Acids Research*, **41**, D1027–D1033.

TINKLE, D., WILBUR, H. and TILLEY, S. 1970. Evolutionary strategies in lizard reproduction. *Evolution*, **24**, 55–74.

VOORHIES, M. R. 1969. *Taphonomy and population dynamics of an early Pliocene vertebrate fauna, Knox County, Nebraska*. Contributions to Geology, Special Paper, **1**, 69 pp.

WEON, B. M. 2015. Tyrannosaurs as long-lived species. *Scientific Reports*, **6**, 19554.

WEON, B. M. and JE, J. H. 2011. Plasticity and rectangularity in survival curves. *Scientific Reports*, **1**, 104.

WERNER, J. and GRIEBELER, E. M. 2011. Reproductive biology and its impact on body size: comparative analysis of mammalian, avian and dinosaurian reproduction. *PLoS One*, **6**, e28442.

WERNER, J. and GRIEBELER, E. M. 2013. New insights into non-avian dinosaur reproduction and their evolutionary and ecological implications: linking fossil evidence to allometries of extant close relatives. *PLoS One*, **8**, e72862.

WESTERN, D. and SSEMAKULA, J. 1982. Life history patterns in birds and mammals and their evolutionary interpretation. *Oecologia*, **54**, 281–290.

WOODWARD, H. N., FREEDMAN FOWLER, E. A., FARLOW, J. O. and HORNER, J. R. 2015. *Maiasaura*, a model organism for extinct vertebrate population biology: a large sample statistical assessment of growth dynamics and survivorship. *Paleobiology*, **41**, 1–25.

ZHAO, Q., BENTON, M. J., XU, X. and SANDER, P. M. 2013. Juvenile-only clusters and behaviour of the Early Cretaceous dinosaur *Psittacosaurus*. *Acta Palaeontologica Polonica*, **59**, 827–833.

ZWEIFEL, R. G. and LOWE, C. H. 1966. The ecology of a population of *Xantusia vigilis*, the desert night lizard. *American Museum Novitates*, **2247**, 1–57.